Chemical Engineering Journal 243 (2014) 473–484

Contents lists available at ScienceDirect

Chemical Engineering Journal

journal homepage: www.elsevier.com/locate/cej

Improved production of fuel oxygenates via glycerol acetylation with acetic acid

M.S. Khayoon [a,b], S. Triwahyono [a,c,*], B.H. Hameed [b], A.A. Jalil [d,e]

[a] Ibnu Sina Institute for Fundamental Science Studies, Universiti Teknologi Malaysia, 81310 UTM Johor Bahru, Johor, Malaysia
[b] School of Chemical Engineering, Engineering Campus, University Sains Malaysia, 14300 Nibong Tebal, Penang, Malaysia
[c] Department of Chemistry, Faculty of Science, Universiti Teknologi Malaysia, 81310 UTM Johor Bahru, Johor, Malaysia
[d] Institute of Hydrogen Economy, Universiti Teknologi Malaysia, 81310 UTM Johor Bahru, Johor, Malaysia
[e] Department of Chemical Engineering, Faculty of Chemical Engineering, Universiti Teknologi Malaysia, 81310 UTM Johor Bahru, Johor, Malaysia

HIGHLIGHTS

- The selective acetylation of glycerol with acetic acid was investigated.
- TAG was produced with very high selectivity of 55% with minimal MAG formed.
- 3%Y/SBA-3 catalyst was the best catalyst to achieve glycerol conversion of 100%.
- The best reaction conditions are; T = 110 °C, time = 2.5 h, catalyst loading = 0.05 g.

GRAPHICAL ABSTRACT

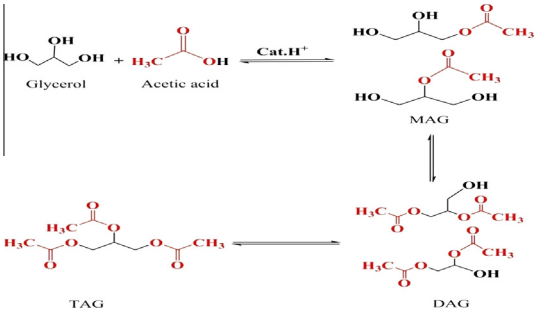

ARTICLE INFO

Article history:
Received 29 October 2013
Received in revised form 11 January 2014
Accepted 13 January 2014
Available online 18 January 2014

Keywords:
Esterification
Triacetyl glycerol
Bioadditives
Yttrium
SBA-3

ABSTRACT

The selective formation of fuel oxygenates via glycerol acetylation with acetic acid over a series of yttrium containing SBA-3 catalysts is reported. The products of glycerol acetylation are mono-, di- and triacetyl glycerol (MAG, DAG, and TAG, respectively) with TAG being the favored. The Y/SBA-3 was prepared by grafting yttrium into the framework of SBA-3. XRD, SAXS, FTIR, SEM–EDX, and surface area and porosity analyzer were used to confirm the properties of the catalysts. The 3%Y/SBA-3 presented unique catalytic performance achieving complete glycerol conversion with corresponding selectivity of 34% and 55% toward DAG and TAG. Over 0.05 g of this catalyst, the reaction conditions were economized to reaction temperature of 110 °C, molar ratio of glycerol to acetic acid of 1:4, and reaction time of 2.5 h. The catalytic activity was mainly attributable to the catalyst' strong acidity and its high surface area with large pore size that facilitate the diffusion of substrates and products. The reaction kinetics model over this catalyst has been developed using experimental data. The stability of the catalyst was examined via leaching and reusability tests through four consecutive batch runs.

1. Introduction

The importance of bio-based fuels to partially replace the fossil fuels and for sustainable growth cannot be overemphasized. Today, the increasing concern about the global warming and the dwindling of global energy supplies have motivated the search for alternative fuels that can partially replace the finite fossil fuels and assist to reduce the noxious emissions. As an alternative to the petro–diesel, biodiesel is acquiring a peerless interest due to its sustainability, low toxicity, high BTUs per gallon and high cetane number, which translated into higher combustion efficiency in an internal combustion engine [1]. Commercially, biodiesel is produced via the catalytic transesterification of triglycerides of fatty

* Corresponding author at: Ibnu Sina Institute for Fundamental Science Studies, Universiti Teknologi Malaysia, 81310 UTM Johor Bahru, Johor, Malaysia. Tel.: +60 75536076; fax: +60 75536080.
E-mail address: sugeng@utm.my (S. Triwahyono).

1385-8947/$ - see front matter © 2014 Elsevier B.V. All rights reserved.
http://dx.doi.org/10.1016/j.cej.2014.01.027

acids (C_{12}–C_{22}) with short chain alcohol such as methanol [2]. Inevitably, the process generates about 100 kg of glycerol as a byproduct for each ton of biodiesel produced [3].

A surplus of glycerol has been produced as a consequence of the biodiesel industry growth, leading to the depreciation of its commercial value and thereby, affecting the industrial feasibility of biodiesel. Therefore, the valorization of this glycerol is intimately intertwined with the new and emerging solutions to ameliorate the biodiesel economy and to cut down its global prices [4]. Recently, great interest has been devoted to convert this polyol into value-added products via different routes such as valorization [5], dehydration [6,7], esterification [8], hydrogenolysis [9], and acetalization [10]. Besides, glycerol acetylation with acetic acid is acquiring special attention due to the industrial importance of the final products. Mono-, di-, and triacetyl glycerol (MAG, DAG and TAG, respectively) are the reaction products, which have found various applications ranging from moisturizers to fuel additives. Particularly, TAG is the most attractive acetin due to its importance as an antiknock agent to gasoline and to its role in improving the cold flow properties and the viscosity of biodiesel [11].

Commercially, glycerol acetylation is performed under batch processes that are catalyzed by conventional BrÖnsted acids like H_2SO_4, H_3PO_4 or HCl as homogeneous catalysts. Such processes are usually accompanied by several technical and environmental drawbacks such as the catalyst separation, product purity, reactor corrosion, and the effluent disposal. As an alternative, different solid acid catalysts including supported heteropolyacids, β-MoO_3/SBA-15, WO_x/TiO_2–ZrO_2, sulfated Zirconia, sulfated activated carbon, and mesoporous silica functionalized with sulfonic acid groups have been employed for this reaction. It was found that the acidity of the catalyst (especially the BrÖnsted acid sites) has a key role toward the selective formation of the favored DAG and TAG products. Despite that these reported catalysts have shown high activity for glycerol acetylation; the low thermal stability and the unsatisfactory selectivity to TAG are still big challenges to the proper design of suitable heterogeneous catalyst for this reaction. In fact, the inevitable water formation in this reaction may lead to weakening the acidic sites [8] and thus, the water–tolerant property of solid acid catalyst is a necessity to perform glycerol acetylation well. In addition, the leaching of the active components to the reaction medium (due to the high polarity of the reaction mixture) is another unresolved problem in many of the previously reported catalytic systems [12,13]. The main reason for the poor hydrothermal stability and the leaching of the metallic species could be assigned to the catalyst preparation techniques. It was reported that catalysts prepared by wet impregnation (WI) method suffered a notable leaching and showed low selectivity to TAG [12]. Contrary to the WI which proceeds through the adsorption (chemi- and/or physisorption) of metal clusters onto the support surface, grafting technique proceeds through surface reaction (condensation, protolysis) of the supports' functional groups (e.g. OH^-) and the metal precursor. Therefore, it is widely accepted that catalyst preparation by grafting of metal species may result in hindering of migration, agglomeration and sintering during the subsequent thermal treatments. Moreover, the catalyst would be of highly dispersed metal ions within its structure or framework. We have reported in our earlier contribution in the preparation and characterization of the yttrium containing SBA-3 catalyst along with its application during the transesterification of glycerol with methyl acetate [14]. Thus, this work emphasizes on the application of an outstanding heterogeneous catalyst of strong BrÖnsted acidity during the selective acetylation of glycerol toward the formation of DAG and TAG under economized process conditions.

2. Materials and methods

2.1. Materials

Anhydrous glycerol of high purity (>99%) was obtained from Sigma, Germany. Glacial acetic acid (100%) and HPLC grade ethanol (99.7%) were supplied by Merck, Malaysia. Tetraethylorthosilicate (TEOS), Yttrium nitrate hexahydrate ($Y(NO_3)_3{\cdot}6H_2O$) of 98% purity, Cetyltrimethyl ammonium bromide (CTMABr), and Pluronic F127 ($EO_{106}PO_{70}EO_{106}$) were purchased from Sigma–Aldrich, Malaysia. Hydrochloric acid (HCl 37%) was obtained from Mallinckrodt, USA. Standard diacetyl glycerol (~50%) and triacetyl glycerol (~99%) were supplied by Sigma–Aldrich, Germany. All reagents were used without further purification. Deionized water was used throughout this work.

2.2. Preparation of the heterogeneous catalysts

In this work, the mesoporous silicate material (SBA-3) was prepared by hydrothermal method and used as catalysts' support. The synthesis details of the mesoporous SBA-3 support and its functionalizing with yttrium species was explained in our previous report [14]. The Y-grafted SBA-3 was prepared by grafting of yttrium species into the lattice of the SBA-3 support, being $Y(NO_3)_3{\cdot}6H_2O$ was added during the support preparation. The obtained catalysts were denoted as (*X*%)Y/SBA-3, where *X* refers to the *Y* mass fraction in the catalyst. To assess the effectiveness of the preparation technique, another group of catalysts prepared by impregnation technique were considered in this study.

2.3. Characterization of the catalysts

The prepared catalysts were characterized for their textural properties (BET surface area, pore volume, and pore size) over Micromeritics ASAP 2020 (USA) surface area and porosity analyzer. X-ray diffraction (XRD) patterns of the pristine SBA-3 and the Y functionalized catalysts (fresh and reused catalysts) were acquired on Bruker D8 Focus X-ray diffractometer (Bruker, Germany) over $10° \leqslant 2\theta \leqslant 90°$. Small angle X-ray scattering (SAXS) diffractograms were used to provide useful information about the repeating unit of the crystallite structure and the interplaner spacing which may be necessary in understanding the crystalline system of ordered materials. The X-ray tube was operated at 40 kV and 30 mA over scattering angle range of $0.5° \leqslant 2\theta \leqslant 5°$ with scan speed of 0.01°/min at room temperature. FTIR spectra of the support and catalyst samples (fresh and reused catalysts) were acquired on Perkin–Elmer System 2000 spectrometer by using the standard KBr technique over the range of 1500–400 cm^{-1}. Scanning electron microscopy (SEM) was used to study the morphology of the synthesized materials using Zeiss Supra TM 35 VP scanning electron microscope (Zeiss, Jena, Germany) coupled with FEI as a source of electrons and accelerated at 300 kV. Energy-dispersive X-ray spectroscopy (EDX) was performed in conjunction with SEM to determine the metallic composition of the catalyst. It is important to mention that the results of SEM characterization for the pristine SBA-3 support and the so modified Y/SBA-3 catalysts were reported in our earlier report [14].

The acidity of prepared catalysts was determined by a neutralization titration procedure. Catalyst powder (0.12 g) was dispersed in 25 mL of 0.02 M NaOH solution and the resulting suspension was gently stirred at room temperature for 48 h. Finally, the mixture was filtered off using membrane filter (0.2 μm pore size) fitted to vacuum system, and the alkali filtrate solution was titrated against 0.02 M HCl solution. The following formula was used to calculate the concentration of acidic sites (*C*):

$$C\ (\mathrm{mmol/g}) = \frac{(\text{Initial moles of NaOH} - \text{Final moles of NaOH})}{\text{Mass of Catalyst (g)}}$$

2.4. Catalytic reactions

The activity of the catalysts was tested in glycerol acetylation with acetic acid in high-pressure Teflon lined stainless steel reactor (100 cm^3) equipped with motor stirrer within temperature range of 80–120 °C. First, 5 g of anhydrous glycerol and 6.2–24.8 mL of acetic acid (corresponding to the varying molar ratios of glycerol to acetic acid) were charged to the reactor. To the reactor, 0.20 g (except in the study of the effect of catalyst weight) of the catalyst was added. The reaction media was heated up to the appropriate reaction temperature and stirred at a rate of 350 rpm. After the catalytic experiment, the catalyst was separated by centrifugation and regenerated by washing it with ethanol and then air dried at 105 °C for 12 h to recuperate its catalytic activity. For comparison, a blank experiment (without adding the catalyst) was performed under the same reaction conditions.

2.5. Analysis of the reaction products

Reaction products were identified using GC/MS Perkin Elmer system (Clarus 600 gas chromatography attached to a Clarus 600T mass spectrometer) equipped with DB-5 column. Aliquots were analyzed by gas chromatography (GC; Shimadzu 2010 plus chromatograph, Japan) equipped with a flame ionization detector (FID) and a ZB5-HT (30 m × 0.25 mm × 0.25 μm) GC capillary column. The products were collected after the completion of each reaction and no sampling was done during the reaction due to the higher reaction temperature (⩾110 °C), a temperature at which acetic acid is in vapor form. The products (MAG, DAG and TAG) selectivity and glycerol conversion were calculated using acetonitrile-based internal standard. About 0.20 μL of the final sample was injected into the column in which the column temperature was initially set at 60 °C (2 min) followed by ramping of 10 °C/min to 260 °C and then heated at 30 °C/min to 300 °C. The FID and injection temperatures were fixed at 350 °C and 250 °C, respectively. Helium at 1.3 ml/min was used as carrier gas. The injection split ratio was 10. Glycerol conversion (X_{gly}) and the product selectivity (S_i) were calculated using the following formulae:

$$X_{gly}(\%) = \frac{\text{moles of glycerol taken} - \text{moles of glycerol unreacted}}{\text{moles of glycerol taken}} \times 100 \quad (1)$$

$$S_i(\%) = \frac{\text{moles of product}_i}{\text{Total moles of products}} \times 100 \quad (2)$$

The calculation of MAG and DAG moles followed the single point internal standard method based on the internal response factor of each component (IRF_i), as follows:

$$\mathrm{IRF}_i = \frac{\mathrm{Area_{IS}} * \mathrm{Moles}_i}{\mathrm{Area}_i * \mathrm{Moles_{IS}}} \quad (3)$$

$$\text{Moles of species } i = \mathrm{Moles_{IS}} * \frac{\mathrm{Area}_i}{\mathrm{Area_{IS}}} * \mathrm{IRF}_i \quad (4)$$

3. Results and discussion

3.1. Catalyst characterization

The characterization results (Textural properties, XRD, SAXS, FTIR, SEM, and EDX) of the catalysts were presented and discussed in our earlier report [14]. In this paper, we report the characterization of the most significant values of such properties for the fresh and spent catalysts (after employing them in glycerol acetylation with acetic acid). For all catalysts, relatively high surface areas were observed (ranged from 1462 for SBA-3 to 1622 m^2/g for 3.5%Y/SBA-3 catalyst) and a pore diameter ranged from 25.4 to 28.6 Å. It was noted that the grafting of Y clusters resulted in catalysts with higher surface area than that of the pristine SBA-3 support, being the 3%Y/SBA-3 catalyst sample possessed a surface area of 1568 m^2/g compared to only 1462 m^2/g for the SBA-3 support. As also stated by Jung et al., the observed increment in the surface characteristics after the grafting of yttrium ions into the lattice of SBA-3 material is caused by an inhibitory effect to the sintering of nano-sized yttrium components [15]. After recycling the 3%Y/SBA-3 catalyst, it was characterized to investigate the effect of the reaction conditions on the textural properties and surface acidity. For the spent catalyst, the surface area decreased from 1568 to 1502 m^2/g, the pore volume from 0.81 to 0.77 cm^3/g, and the pore diameter from 25.4 to 25.1 Å. These changes in surface properties are minute and could strongly assert the mechanical stability of the catalyst particles under the stirring conditions.

Out of all catalysts, the 3%Y/SBA-3 catalyst has possessed the strongest BrÖnsted acidity of 1342 μmol/g. And it was observed that the surface acidity of this catalyst reduced to 1288 μmol/g after the fourth recycle. This can possibly be attributed to the hydration effect of the co-produced water from the acetylation reaction.

The XRD patterns of the pristine SBA-3 and the so-developed 3%Y/SBA-3 catalyst were presented and discussed in our previous report [14], but a comparison was made with the spent 3%Y/SBA-3 catalyst after reusing it in glycerol acetylation (Fig. 1a). This comparison is important to understand the effect of the co-produced water on the catalyst system. Fig. 1b shows the SAXS diffractograms of the fresh and spent 3%Y/SBA-3 catalyst, which were explained in that report. The SAXS patterns showed three well-resolved Bragg angles in hexagonal lattice symmetry, indicating the ordered structure of SBA-3 material before and after the modification with yttrium species. This observation is corroborated with the physical explanation reported elsewhere [16]. X-ray investigations were also made to evaluate the stability of the spent 3%Y/SBA-3 crystalline structure, Fig. 1. No serious changes were observed in both patterns compared to that of fresh 3%Y/SBA-3 catalyst, indicating the hydrothermal stability of this catalyst under the reaction conditions.

The synthesized catalysts (fresh and spent 3%Y/SBA-3) were also characterized by FTIR analysis to investigate the chemical interactions between the support surface and the guest Y species (Fig. 2). The FTIR spectra of these catalysts have showed some characteristics IR absorptions as below:

IR band	Attributable to the
463 and 865 cm^{-1}	symmetric Si–O–Si tetrahedron in the structural siloxane bond [16],
1077 cm^{-1}	asymmetric Si–O–Si tetrahedron in the structural siloxane bond [17],
962 cm^{-1}	stretching vibration modes of Y–O–Si, [15,18]
577 cm^{-1}	presence of Y–O bonding within the structure [19],

It is obvious from the nature of the chemical bonding that the structure of the fresh and the spent 3%Y/SBA-3 catalyst has contained the active yttrium species as building components. This could evidently assert the stability of the catalytic activity of this catalyst during glycerol acetylation with acetic acid. By interpreting

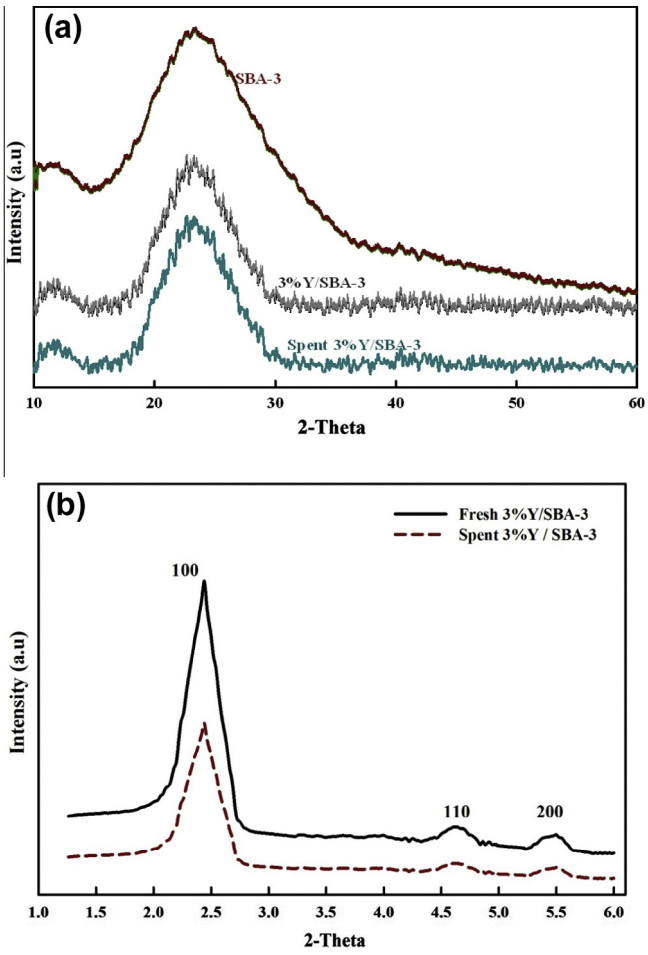

Fig. 1. XRD patterns of SBA-3, fresh and spent 3%Y/SBA-3 catalyst.

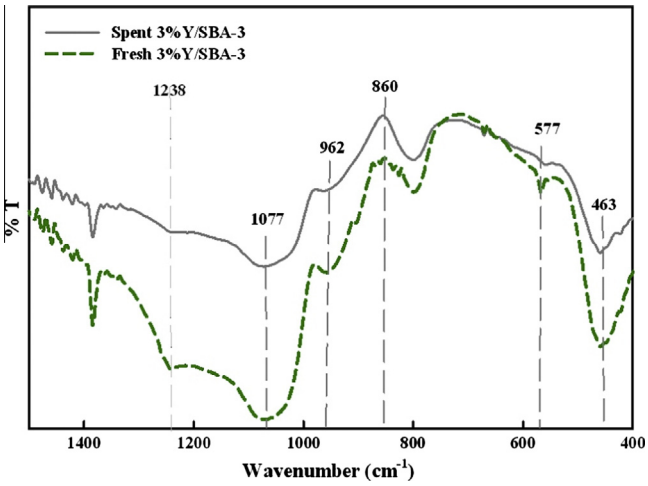

Fig. 2. FTIR spectra of SBA-3, fresh and spent 3%Y/SBA-3 catalyst.

the results of XRD and FTIR analysis of the spent catalyst, one can trustfully describe this catalyst as "water–tolerant", due to its resistance to the hydrolysis effects of the co-produced water.

SEM images of the synthesized materials (SBA-3, fresh and spent 3%Y/SBA-3 catalysts) are presented in Fig. 3a–c. The obtained images confirmed the spheroid morphology of the SBA-3 material and clearly showed the attachment of Y species to the support structure. It was difficult to identify the distribution of the guest elemental components over the support surface due to the aggregation of the catalyst particles in bunch clusters. SEM image of the spent 3%Y/SBA-3 catalyst showed no appreciable morphological changes after the acetylation reaction (Fig. 3c). The elemental content of the fresh and the spent 3%Y/SBA-3 catalyst was determined with EDX. Table 1 summarizes the metallic profile of this catalyst. It is obvious that the loading of Y in this catalyst is 2.96 wt.%, which found to be close to the theoretical value of 3 wt.%. This could merely assure the precision of the preparation procedure and supports the claim of the stability of the obtained catalyst structure under the reaction conditions.

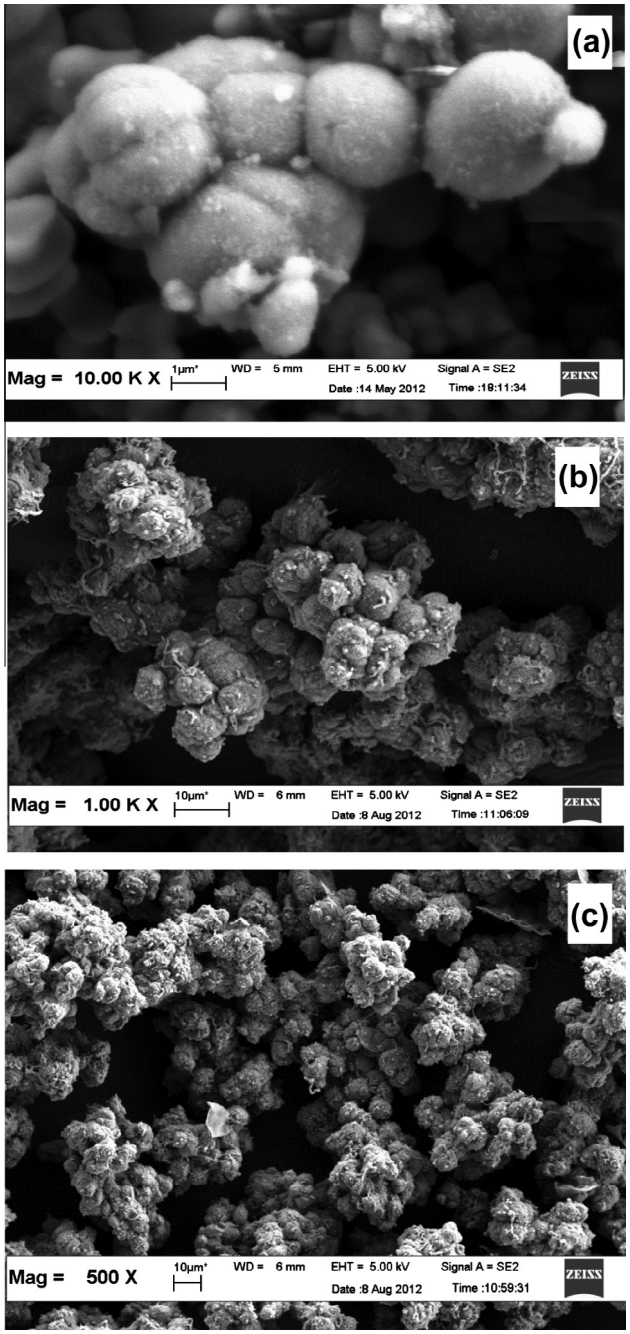

Fig. 3. SEM images of (a) SBA-3, (b) Fresh 3%Y/SBA-3 catalyst, and (c) Spent 3%Y/SBA-3 catalyst.

Table 1
EDX elemental analysis results for the fresh and spent 3%Y/SBA-3 catalyst.

Catalyst	Elemental content (%)					
	Theoretical			By EDX		
	Y	Si	O	Y	Si	O
3%YSBA-3	3	63	34	2.96	65.4	31.64
3%YSBA-3R	–	–	–	2.89	64.8	32.23

3.2. Catalytic activity: acetylation of glycerol with acetic acid

The catalytic performance of variously loaded Y/SBA-3 catalysts was evaluated during glycerol esterification by means of glycerol conversion and product selectivity. The path of such a reaction involves the conversion of glycerol to MAG, whereas DAG and TAG products were formed through consecutive acetylation reactions [20]. This mechanism suggests that a product with a lower MAG content will be of higher DAG and/or TAG content (based on high glycerol conversion). Scheme 1 illustrates the reaction pathway of glycerol acetylation with acetic acid over heterogeneous catalyst.

A series of SBA-3 catalysts with varying loading of Y (1–3.5 wt.%) were employed to facilitate the acetylation reaction of glycerol with acetic acid. The results of the catalytic activity are summarized in Table 2. For comparison to the grafted catalysts, another series of Y/SBA-3 catalysts were prepared by impregnation of Y on SBA-3 support. For the grafted samples, it was noticed that the catalytic activity increases as the amount of yttrium grafted increases up to the level of 3 wt.%. While the catalyst with 3.5 wt.% of Y possessed lower catalytic activity than the latter. This might be explained by the number of accessible active sites, which increases with increasing the Y concentration up to the level of anchoring points saturation. Therefore, the catalyst with 3.5 wt.%Y showed a decrease in catalytic activity, leading to the conclusion that 3 wt.%Y represents the optimum metal loading. Furthermore, the performance of the 3.5%Y/SBA-3 catalyst did not bring about the desired effect as the reaction could have been limited by the mass transfer during the reaction.

The obtained selectivity to DAG and TAG over 3%Y/SBA-3 catalyst were found to be higher than that obtained with SBAH-15(15) catalyst [21], which might be ascribed to the selective behavior of yttrium during the consecutive acetylation reactions of MAG to DAG and TAG. The 3%Y/SBA-3 was readily active, achieving complete conversion of glycerol with corresponding selectivity of 11%, 34% and 55% toward MAG, DAG and TAG, respectively. The economized reaction conditions were; reaction temperature of 110 °C, molar ratio of glycerol to acetic acid of 1:4, and reaction time of 2.5 h.

Physically, the performance of 3%Y/SBA-3 catalyst could be explained by the extremely high surface area (1568 m^2/g) and the stability of the crystalline structure of the SBA-3 material after the grafting of Y species (as also proved by SAXS results, [14]). The high surface area of the support has resulted in the uniform prevalence of Y species into its framework. It is worthy to mention that the amount of $Y(NO_3)_3$ used in the 3%Y/SBA-3 catalyst preparation was decomposed to synergistically interlocked Y–O–Si and Y–O components, that are therefore believed to be the active components within the structure of this catalyst.

The catalytic performance of 3%Y/SBA-3 was compared with that of other catalysts (AC-SA5 and SBAH-15(15)), which have been reported in our earlier contributions [21,22]. It can be simply observed that the catalytic activity increases in the order of AC-SA5 < SBAH-15(15) < 3%Y/SBA-3. Apart from the effects of the reaction conditions, the observed trend could be explained by the effects of group of factors (physical and chemical). Physically, it was found that the catalyst surface area increases in the same trend which gives a logical explanation that this parameter strongly affects the catalytic activity, as the acetylation of glycerol is a consecutive reaction and higher surface area could favor the second and the third reactions [23,24]. In addition, the crystallinity (which refers to the degree of structural order in a solid) of the catalyst was found to be more ordered for 3%Y/SBA-3 catalyst than SBAH-15(15) catalyst (as proved and discussed by XRD and SAXS results) and surely of AC-SA5 since it is a highly amorphous material.

Moreover, the intra-microporosity introduced within the *p6m* wall structure of the 3%Y/SBA-3 catalyst was higher than that of *p6mm* structure of SBAH-15(15) catalyst which is possibly related to the crystal phase density that was found to be higher for the *p6mm* material. This microporosity is importance especially for the internal diffusion limited reactions (as the case of glycerol

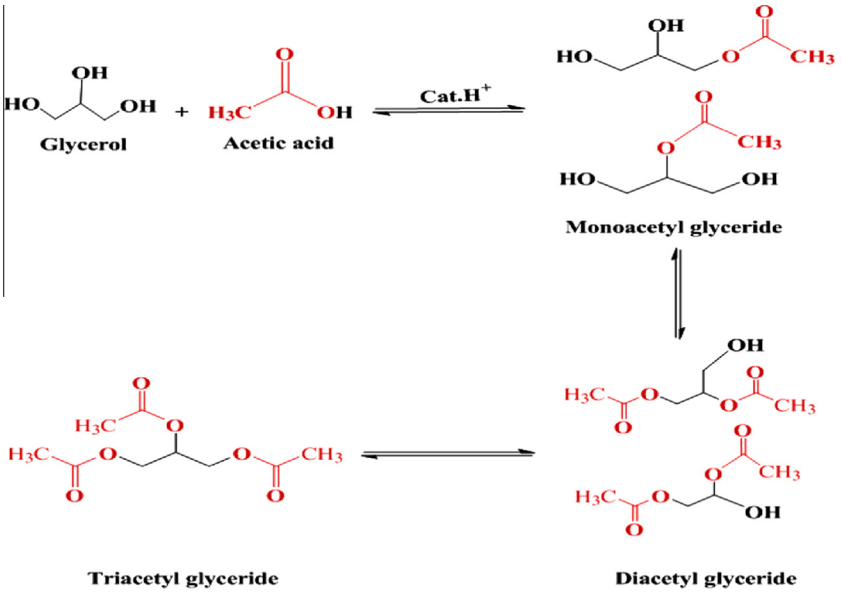

Scheme 1. Glycerol acetylation with acetic acid.

Table 2
Comparison of the catalytic activity of different silica based heterogeneous catalysts with different MPA concentrations during glycerol acetylation with acetic acid using variant glycerol to acetic acid molar ratio (1:4; 1:6; 1:8) at 110 °C after 3 h.

Catalyst	Conversion (%)			Selectivity (%)								
				MAG			DAG			TAG		
	1:4	1:6	1:8	1:4	1:6	1:8	1:4	1:6	1:8	1:4	1:6	1:8
Blank test	20	27	31	71	54	43	28	42	52	1	4	5
1% Y/SBA-3	65	74	76	95	91	75	5	8	20	0	1	5
2%Y/SBA-3	68	75	79	82	78	71	11	13	12	7	9	17
2.5%Y/SBA-3	82	85	87	54	43	42	26	28	28	20	29	30
3%Y/SBA-3	100	100	97	11	10	19	34	35	25	55	55	56
3.5%Y/SBA-3	94	95	86	24	23	20	39	40	29	37	37	51
1%Y/SBA-3 (Im)	79	90	91	30	22	21	47	53	51	23	25	38
3%Y/SBA-3 (Im)	88	96	96	19	15	12	50	47	47	31	38	41
SBAH-15(15)[a]	–	100	–	–	14	–	–	67	–	–	19	–
AC-SA5[b]	–	–	91	–	–	38	–	–	28	–	–	34

[a] Ref. [21].
[b] Ref. [22].

acetylation) and thereby, the 3%Y/SBA-3 catalyst was found to be more active than SBAH-15(15) catalyst toward the formation of higher glycerol acetates (DAG and TAG). These observations are in good agreement with those reported in the literature [25–28].

On the other hand, several chemical parameters affect the rate of glycerol acetylation with acetic acid; being the steric hindrance and the interaction with the active sites on the catalyst surface as the two main factors. Indeed, glycerol acetylation can be an example for the steric hindrance between adjacent groups which restrict torsional bond angles [23,28]. Thence, a well-engineered catalytic material with high surface area could effectively contribute toward reducing this hindrance by providing extra catalytic sites that enhance the interaction between the reactive molecules. The interaction of the reactive molecules with the active sites could also be another factor, as the catalytic site may be buried within a large molecule and leading to the active site decease [28,29]. Thence, the grafting of the active metal species within the structure of the support may assist in decreasing the number of deceased sites, as these sites will not be on the catalyst surface only.

For the uncatalyzed experiments, the value of glycerol conversion may be explained according to the collision theory which presumes that the collisions can only occur when certain molecules of the reactants hit with each other. The chemical reaction can only take place by the successful collisions which require having a certain amount of energy, at the moment of impact to break the pre-existing bonds and form all new bonds. Involving a catalyst into the reaction media might reduce the activation energy required for the chemical reaction to occur, and hence more collisions have sufficient energy for the reaction to take place. The reaction rate therefore increases.

3.3. Effect of reaction parameters

3.3.1. Effect of catalyst weight

Fig. 4 shows the results for the reaction profile studied using varying amounts of 3%Y/SBA-3 catalyst. The reactions were carried out using a molar ratio of glycerol to acetic acid of 1:4 at 110 °C for 3 h. The conversion of glycerol increased in the same trend with AC-SA5 and SBAH-15(15) catalysts, but the selectivity to DAG and TAG was much higher than those previously observed for AC-SA5 and SBAH-15(15) catalysts (Table 2). It is interesting to observe that the formation of TAG was noted with all of the catalyst dosages. This might be explained by the selective behavior of Y components in the 3%Y/SBA-3 catalyst. Over this catalyst, the selectivity to TAG (55%) was higher than those obtained using

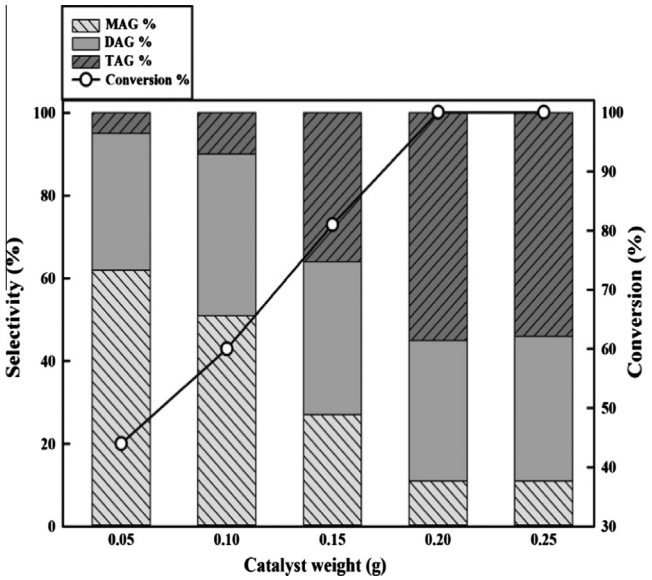

Fig. 4. Effect of catalyst weight (g). Reaction conditions: molar ratio of glycerol/acetic acid: 1:4; reaction temperature: 110 °C; reaction time: 3 h.

other catalysts (over AC-SA5 was 34% and over SBAH-15(15) was 19%), which evidently explains the selective behavior of Y and its activity during the consecutive acetylation reactions. The conversion of glycerol was 44% at the catalyst weight of 0.05 g (corresponding to 1 wt.% catalyst loading with respect to glycerol weight), but it gets 100% as the catalyst amount increased to 0.20 g. In conclusion, yttrium clusters grafted in SBA-3 support showed better catalytic activity than β-MoO_3 attached to SBAH-15 support during the acetylation of glycerol.

3.3.2. Effect of molar ratio

The effect of glycerol/acetic acid molar ratio was investigated using the proportions 1:4, 1:6 and 1:8 at a fixed reaction temperature of 110 °C. An excess of carboxylic acid utilized in acetylation reaction might shorten the time required to reach reaction equilibrium and provide more acetylating agent which enhances the formation of DAG and TAG through the consecutive acetylation reactions [30]. Table 2 also presents the results of glycerol conversion and product selectivity during the acetylation of glycerol with acetic acid using variant molar ratios of glycerol/acetic acid over Y grafted SBA-3 catalyst. The 3%Y/SBA-3 catalyst was reliably active at low glycerol/acetic acid molar ratio of 1:4, achieving complete

conversion of glycerol with corresponding selectivity of 11%, 34%, and 55% toward MAG, DAG, and TAG, respectively. On the contrary to the AC-SA5 and SBAH-15(15) catalysts, the selectivity to DAG and TAG did not increase as the molar ratio increased to 1:6 over the 3%Y/SBA-3 catalyst. As the molar ratio increased to 1:8, a minute decrease in glycerol conversion and a notable decrease in DAG selectivity were observed, which might be explained by the effect of the excess acid added that enhanced the backward reaction of glycerol to MAG. The decrease in DAG selectivity can be explained by the hydrolysis effect of the co-produced water, as also observed with SBAH-15(15) catalyst. The results of glycerol conversion and product selectivity for glycerol acetylation with acetic acid over the 3%Y/SBA-3 catalyst can be considered as the best ever achieved compared to those reported in the literature. The catalytic performance of 3%Y/SBA-3 catalyst at a low molar ratio might be ascribed to its extreme textural characteristics and the stability of its crystal phase, as confirmed by the results of catalyst characterization (BET, XRD and SAXS). The presence of Y–O bonds within this catalyst may also define the nature of the active sites within this catalyst, as also proved by FTIR results.

The reaction of alcohol with acetic acid has been proposed as an equilibrium-limited reaction [31]. To displace the reaction to equilibrium, two possible routes were widely used: first by reactive distillation to displace the co-produced water from the reaction medium and second by employing an excess of carboxylic acid [32]. In this work, the rate of acetylation was accelerated by using excess acetic acid with strong acid catalysts.

3.3.3. Effect of reaction time

The effect of reaction time on the reaction profile over the 3%Y/SBA-3 catalyst was equally investigated and the results are shown in Fig. 5. After 30 min of the reaction, 62% of glycerol was converted to MAG and DAG only. The reaction went to completion after 60 min, as all glycerol converted to acetylated products. The selectivity to MAG was observed to decrease as the reaction proceeded, whereas that of DAG kept increasing up to 90 min. The formation of TAG was started after 30 min, which could be attributed to the direct acetylation of MAG to TAG. After 90 min, the formation of TAG has been initiated by the acetylation of some of the produced DAG, as indicated by the dropped curve of DAG after 90 min. Thereafter, the selectivity to MAG was decreased steeply due to its expense by the second acetylation toward DAG and possibly to TAG. This behavior could help in explaining the reaction pathway over a 3%Y/SBA-3 catalyst, which was observed to slightly differ than those over AC-SA5 and SBAH-15(15) catalysts, which assumed the formation of the acylium ion intermediate and the formation of TAG was started after 30 min. In this pathway, the formation and disappearance of that intermediate were faster, since the formation of MAG, DAG, and TAG was clearly noted after 30 min with no by-products detected. In conclusion, reaction time of 150 min was required to achieve complete glycerol conversion with 89% of combined selectivity to DAG and TAG over a 3%Y/SBA-3 catalyst, and found to be shorter than that required with SBAH-15(15) catalyst to achieve complete glycerol conversion with 84% of the combined selectivity.

3.3.4. Effect of reaction temperature

The effect of reaction temperature on glycerol acetylation catalyzed by 3%Y/SBA-3 catalyst was also equally investigated and the obtained results are presented in Fig. 6. Increasing the reaction temperature from 90 to 110 °C resulted in a substantial increase in glycerol conversion from 65% to 100% and further heating did not affect this value. It was found that the formation of TAG is a temperature dependent reaction, being the selectivity to TAG at temperatures of lower than 90 °C was almost less than 7%. This observation is logical and corroborating with others reported elsewhere [28,33]. The research community has devoted serious attention to reduce the reaction temperature and attain high DAG and TAG productivity either by employing other acetylating agents or by using different catalytic materials [8,3].

3.4. Activity stability tests

3.4.1. Leaching test

The leaching test of the metallic species from the catalyst structure was implemented according to the hot filtration method. The 3%Y/SBA-3 catalyst was immersed in a known volume of acetic acid and the mixture was then heated to the reaction temperature (110 °C) and kept under constant stirring rate of 530 rpm for 3 h. Afterward the catalyst was removed and known mass of glycerol

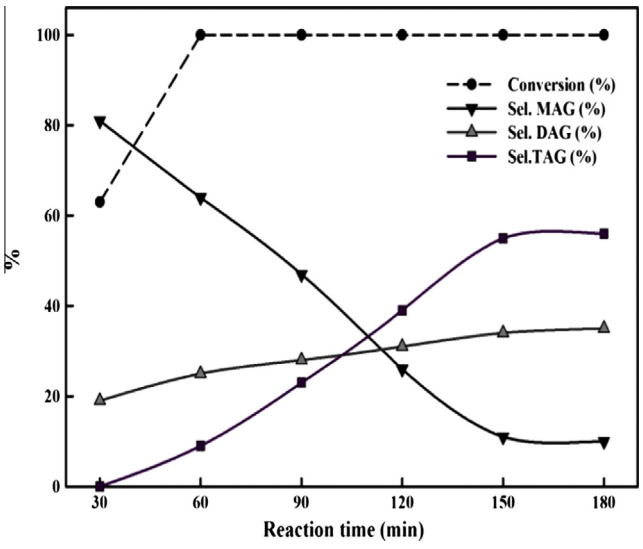

Fig. 5. Effect of reaction time during glycerol acetylation over 3%Y/SBA-3 catalyst. Reaction conditions: molar ratio of glycerol/acetic acid: 1:4; reaction temperature: 110 °C.

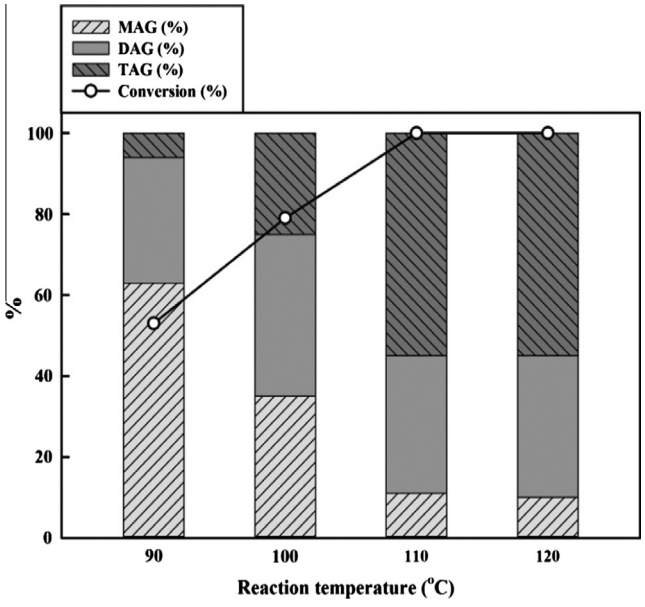

Fig. 6. Effect of reaction temperature on glycerol conversion (%) and selectivity (%) during glycerol acetylation over 3%Y/SBA-3 catalyst. Reaction conditions: molar ratio of glycerol/acetic acid: 1:4; reaction time: 2.5 h.

was added to each reactor. The acetic acid–glycerol mixtures were subjected to the best reaction conditions, allowing them to react in the absence of the catalysts. Thereafter, the reaction samples were analyzed to determine the conversion of glycerol and comparing these values to that obtained from blank test. The 3%Y/SBA-3 catalyst has showed no appreciable leaching of the metallic components to the liquid phase, which strongly validate the claim for its stability.

3.4.2. Reusability tests

The 3%Y/SBA-3 catalyst was equally subjected to various experimental tests to investigate its stability. For instance, after each batch run, the catalyst was separated and thoroughly washed with methanol until all traces of adhering liquids were removed. Fig. 7 shows the obtained results for the tests over four repeated cycles. As would be observed from the figure, the catalytic activity was stable up to the third run, but notably decreased in the fourth recycle, as indicated by the decreased conversion of glycerol from 100% to 80% and the selectivity to TAG from 55% to 50%. This behavior could be explained due to the effects of reaction conditions and the mass transfer limitations. It can be clearly seen that 3%Y/SBA-3 catalyst has met some criteria of the research goals in terms of leaching and reusability and could possibly be commercialized for industrial scale. Therefore, it was believed that the surface area could be the reason for the improved catalytic activity of 3%Y/SBA-3 catalyst. The surface acidity was determined to be 1342, 960, and 890 μmol/g for 3%Y/SBA-3 catalyst, SBAH-15(15), and AC-SA5 catalysts respectively. The surface acidity is therefore considered as a prominent factor explaining the trend catalytic activity increase.

3.5. Kinetics study and determination of reaction kinetics parameters

3.5.1. Reaction kinetic model and analysis of the kinetics data

The experimental kinetics study of glycerol acetylation with acetic acid was carried out by carrying out the reaction at various temperatures and collecting the reaction samples at varying time intervals. The other parameters like the initial reactants molar ratio and catalyst amount that may affect the kinetics study were kept constant.

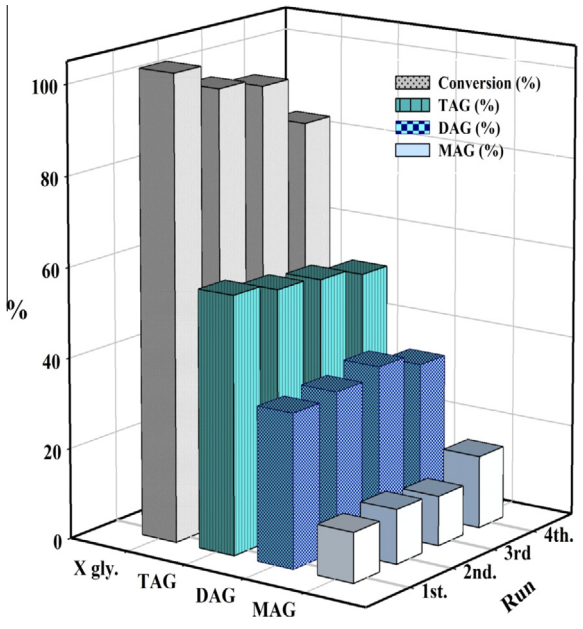

Fig. 7. Reusability test performed for 3%Y/SBA-3 catalyst. Reaction conditions for each run: catalyst loading: 0.20 g; reaction time: 2.5 h; reaction temperature: 110 °C; molar ratio of glycerol/acetic acid: 1:4. MAG: monoacetyl glyceride; DAG: diacetyl glyceride; TAG: triacetyl glyceride; X_{gly}: glycerol conversion (%).

As the acetylation reaction was performed by reacting glycerol (***G***) with excess amounts of acetic acid (***B***), a pseudo-first order reaction was proposed. The generalized reaction rate can be expressed as $-r_G = -dC_G/dt = k_1 C_G^{\alpha} C_B^{\beta}$. Since ***B*** is present in excess, its concentration has virtually remained constant during the stated reactions. Therefore, the reaction's rate depends in particular on the concentration of glycerol (G) as it is the limiting reactant. Taking into account both the external and internal mass transfer resistance, the rate of disappearance of glycerol can thus be determined using the proposed pseudo-first order reaction rate equation, as follow

$$-\frac{dC_G}{dt} = k_m a_m (C_{G,b} - C_{G,s}) \tag{5}$$

where k_m, a_m, $C_{G,b}$ and $C_{G,s}$ are the mass transfer coefficient, external surface area of the catalyst, concentration in the bulk liquid and concentration on the catalyst surface, respectively. By assuming that the reaction rate on the catalyst surface is much faster than that in the bulk liquid system, the reaction therefore is under mass transfer limitations and not under kinetic control, hence it is the rate determining then $C_{G,s} = 0$. Since the external surface area of the catalyst and the mass transfer coefficient are constant within the reaction system, then $k_1 = k_m\, a_m$. Thus, the differential form of the reaction rate equation can be written as:

$$-\frac{dC_G}{dt} = k_1 (C_G) \tag{6}$$

and by integration gives

$\ln\left(\frac{C_G}{C_{G0}}\right) = -k_1 t$, and since $C_G = C_{Go}\,(1 - X_G)$; then:

$$-\ln(1 - X_G) = k_1 t \tag{7}$$

where X_G is the fractional conversion of glycerol. The plot of $-\ln(1 - X_G)$ versus t will be a straight line with a slope of (k_1), from which k_m was calculated by neglecting the external mass transfer limitations. The plots of glycerol concentration, C_G versus time for the different temperatures were considered to determine the reaction rate order.

3.5.2. Experimental kinetics study over 3%Y/SBA-3 catalyst

Studies on the reaction kinetics study of glycerol acetylation with acetic acid are rarely found in literature [34,35]. The previous studies were performed using sulfuric acid as a homogeneous catalyst. No peer studies have been reported for studying the kinetics of this reaction over heterogeneous catalyst. The knowledge of kinetics study is necessary as it help to determine the reaction order, reaction rate, and the activation energy. Thence, the well-known Arrhenius model with account for the batch constant volume reactor system is employed to determine the rate law parameters. The determination of the reaction order, and the specific reaction rate constant (k) is usually achieved by measuring the concentration as a function of time and analyzing the obtained data using the integral, differential or the least square method.

In this work, it was assumed that glycerol aetylation behaves like a first order irreversible reaction, in which glycerol was assigned as the limiting reactant. The plots of C_G against t at different temperatures are presented in Fig. 8. As expected, glycerol concentration was observed to decrease as the reaction time prolonged. According to the plots, the order of the reaction was found to follow zero and pseudo-first orders with well fitted data which indicate a shift from lower to higher order as C_G drops in the system. The overall reaction rate was found to follow the pseudo-first order.

The experimental data of fractional glycerol conversion (X_G) were plotted in the form of $-\ln(1 - X_G)$ against the reaction time

(t) at different temperatures, as shown in Fig. 9a–c. The plots followed a linear trend with a correlation factor, R^2, of 0.983 and with a slope value of 0.0242 (min^{-1}) with respect to Fig. 9b. The presence of acetic acid in an excess amount favored the forward (irreversible) reaction, which implies the presence of glycerol in low concentration in the equilibrium composition. To this end, the surface reaction can be considered as the rate limiting step (RLS). The reaction required an excess of acetic acid (glycerol: acetic acid of 1:4) to compensate its slow rate and it would be expected under this condition, the reaction order with respect to acetic acid approaches zero. The above observation is in good agreement with literature reports [34,35]. They observed that the reaction order with respect to acetic acid approaches zero and thus, the rate equation depends only on glycerol concentration.

According to Fig. 9a–c, three possible values of k_1 could be obtained, that are $k_1 = 0.0188$ (min^{-1}), $R^2 = 0.993$; $k_1 = 0.0242$ (min^{-1}), $R^2 = 0.983$; and $k_1 = 0.0228$ (min^{-1}), $R^2 = 0.986$. Arrhenius equation was then used to calculate the activation energy for the acetylation reaction of glycerol with acetic acid, that is

$$\ln\frac{k_1}{k_2} = -\frac{E_a}{R}\left(\frac{1}{T_1} - \frac{1}{T_2}\right) \tag{8}$$

where R is the universal gas constant (8.314 J mol^{-1} K^{-1}). The overall acetylation reaction of glycerol with acetic acid would be assumed to behave like a one-step reaction. Thus, the reaction rate ($-r_G$) for the reversible reaction shown in Scheme 2, is given by:

$$-r_G = -\frac{dC_G}{dt} = k_f C_G C_B^9 - k_b C_M C_D C_T \tag{9}$$

where C_B, C_M, C_D, and C_T referring to concentrations of acetic acid, MAG, DAG, and TAG, respectively. Since the concentration of glycerol relates to the fractional conversion (X_G), by the relation $C_G = C_{Go}(1 - X_G)$, the initial concentration of acetic acid is denoted by C_{Bo}. Thus,

$C_B = C_{Bo} - 9C_{Go}X_G$, $C_M = C_{Go}X_G$, $C_D = C_{Go}X_G$, and $C_T = C_{Go}X_G$, it produces:

$$-r_G = C_{Go}\frac{dX_G}{dt} = k_f C_{Go}(1 - X_G)(C_{Bo} - 9C_{Go}X_G) - k_b(C_{Go}X_G)^3 \tag{10}$$

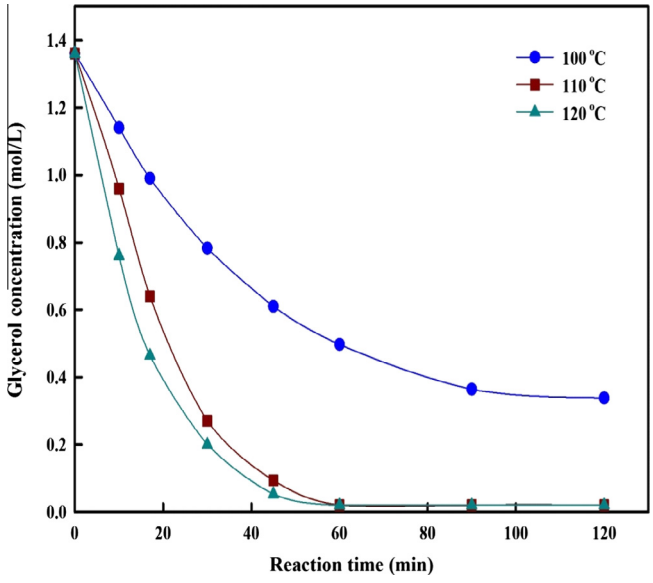

Fig. 8. Plots of glycerol concentration versus time at different temperatures. Reaction conditions: molar ratio of glycerol/acetic acid: 1:4; catalyst amount: 0.40 g; reaction temperature: 110 °C; reaction time: 2.5 h.

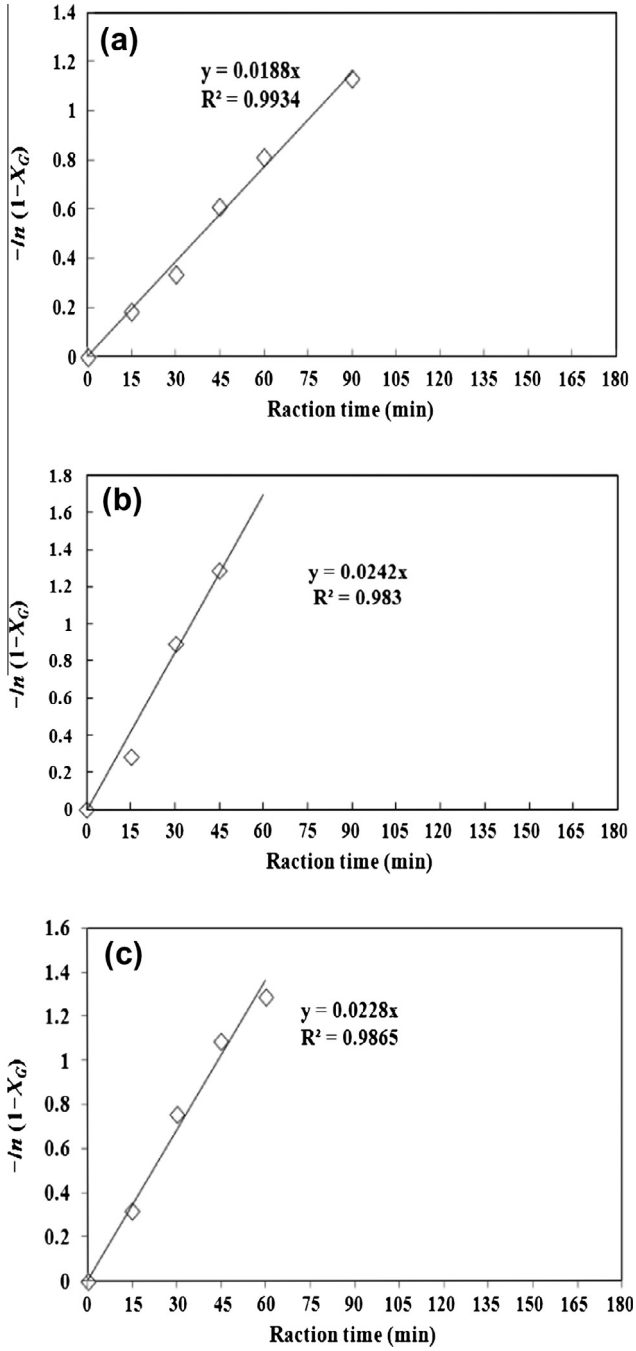

Fig. 9. Plots of $-\ln(1-X_G)$ versus reaction time at: (a) 100 °C; (b) 110 °C; and (c) 120 °C.

$$C_3H_8O_3 + 9\,C_2H_4O_2 \rightleftharpoons C_5H_{10}O_4 + C_3H_5OH(CH_3COO)_2 + C_9H_{14}O_6 + 4H_2O$$

Scheme 2. The overall reversible reaction of glycerol with acetic acid.

At equilibrium, $r_G = 0$, and $X_G = X_{Ge}$, therefore Eq. (10) becomes:

$$0 = k_f C_{Go}(1 - X_{Ge})(C_{Bo} - 9C_{Go}X_G) - k_b(C_{Go}X_{Ge})^3 \tag{11}$$

where k_f and k_b are the forward and the backward rate constants, respectively. Since the equilibrium constant (k_e) represents the ratio between the forward and the backward rate constants, and by solving Eq. (11) for k_e, it gives:

Table 3
The calculated values of the kinetic model parameters.

Parameters	Symbol/units	Calculated value
Pre-exponential factor	A (min^{-1})	0.883×10^3
Activation energy	E_a (kJ/mol)	21.54
Gibbs free energy	ΔG (J/mol)	−676.82
Equilibrium constant	k_e	1.17
Diffusivity	D_e	4.22×10^{-8}
Thiele modulus	φ_s	0.462
Effectiveness factor	η	0.971
Adsorption coefficient	θ_{Ads}	0.38
Adsorption constant	K_A (cm^3/mol)	0.085

$$k_e = \frac{C_{Go}^2 X_{Ge}^3}{(1 - X_{Ge})(C_{Bo} - 9C_{Bo}X_{Ge})} \tag{12}$$

Based on the herein derived kinetic models, the corresponding values of the kinetics and thermodynamics parameters were calculated for the acetylation process at the reaction conditions using POLYMATH 5.1 software and presented in Table 3.

3.5.3. Rate limiting step

Derivation of the kinetic model:

The acetylation reaction of glycerol with acetic acid is a sequential reaction that encompasses three consecutive steps; conversion of glycerol to MAG, MAG to DAG, and DAG to TAG. The overall chemical reaction equation is represented in Scheme 2, which can also be rewritten in coded form as:

$$G + 9B \rightleftharpoons M + D + T + 4W \tag{13}$$

where G is the glycerol, B is acetic acid, M is monoacetyl glycerol, D is diacetyl glycerol, and T is the triacetyl glycerol.

The proposed mechanisms for the formation of M, D, and T are explained in serial steps based on the Langmuir–Hinshelwood kinetics with the surface reaction being the rate limiting step and neglecting the concentration of the co-produced water. When writing the rate laws for these steps, we treat each step as an elementary reaction, the reactions would be:

Adsorption:

1. Glycerol (G) will first attack the vacant site (S) on the catalyst surface

$$G + S \underset{k_1}{\overset{k_1'}{\leftrightarrows}} G.S \text{ (Adsorption of glycerol on the surface)}$$

$$r_G = k_1 C_G \overline{C}_v - k_1' \overline{C}_G \tag{14}$$

where $\overline{C}_v$ is the concentration of vacant sites over the catalyst surface, and $\overline{C}_G$ is the concentration of glycerol on the catalyst surface.

2. Adsorption of acetic acid on the surface

$$B + S \underset{k_1}{\overset{k_1'}{\leftrightarrows}} B.S$$

$$r_G = k_1 C_B \overline{C}_v - k_1' \overline{C}_B \tag{15}$$

Accordingly, the net rate of adsorption (r_G) related to the molar concentration of total sites ($\overline{C}_m$), becomes

$$r_G = k_1 C_G(\overline{C}_m - \overline{C}_v) - k_1' \overline{C}_G \tag{16}$$

$$r_G = k_1 \left[C_G \overline{C}_v - \frac{\overline{C}_G}{K_{ads}} \right] \tag{17}$$

In case of simultaneous reaction is considered and species G and B are adjacent to each other. Thus, the adsorption process and surface reactions will occur according to the type given below.

3. $G.S + B \xrightarrow{k_2} M.S$ (The formation of MAG)

$$r_s = k_2 \overline{C}_G C_B - k_2' \overline{C}_M \tag{18}$$

$M.S + B \xrightarrow{k_3} D.S$ (The formation of DAG)

$$r_s = k_3 \overline{C}_M C_B - k_3' \overline{C}_D \tag{19}$$

$D.S + B \xrightarrow{k_4} T.S$ (The formation of TAG)

$$r_s = k_4 \overline{C}_D C_B - k_4' \overline{C}_T \tag{20}$$

In the case that the reaction takes place between adsorbed G and adsorbed B, then

4. $G.S + B.S \xrightarrow{k_3} M.S + S$

From the reaction above, it is assumed that only the adsorbed G immediately adjacent to adsorbed B will react to yield the product. Thus, the net rate of the reaction can be expressed by:

$$r_s = k_3 \overline{C}_G \frac{\overline{C}_B}{\overline{C}_m} - k_3' \overline{C}_M \frac{\overline{C}_v}{\overline{C}_m}$$

$$r_s = \frac{k_3}{\overline{C}_m} \left[\overline{C}_G \overline{C}_B - \frac{1}{K_s} \overline{C}_M \overline{C}_v \right] \tag{21}$$

The surface reaction will occur at equilibrium ($r_s = 0$) if the resistance is neglected, and then:

$$K_s = \left(\frac{\overline{C}_M \overline{C}_v}{\overline{C}_G \overline{C}_B} \right) \tag{22}$$

Desorption:

The products desorption from the process of glycerol acetylation takes place in the following form:

5. $M.S + D.S + T.S \xrightarrow{k_4'} M + D + T + 3S$

$$r_M = k_4 \overline{C}_M - k_4 C_M \overline{C}_v \tag{23}$$

$$r_D = k_4 \overline{C}_D - k_4 C_D \overline{C}_v \tag{24}$$

$$r_T = k_4 \overline{C}_T - k_4 C_T \overline{C}_v \tag{25}$$

The equations of desorption rate show that it is reversible to the adsorption process. The concentrations of the adsorbed species can be obtained considering that the reaction rate constant for the formation of intermediates is large compared to the reaction rate. Therefore,

$$\frac{r_{ads}}{r_d} \approx \frac{k_{ads}}{k_d} \approx 0 \tag{26}$$

Which represents pseudo-equilibrium, then:

$$\overline{C}_{G_e} = K_G C_G \overline{C}_v \tag{27}$$

With $k_4 = k_d$, at equilibrium, $r_M = r_D = r_T = 0$ and the equations of desorption give the expressions for $\overline{C}_M$, $\overline{C}_D$ and $\overline{C}_T$.

$$\overline{C}_M = K_d C_M \overline{C}_v \tag{28}$$

$$\overline{C}_D = K_d C_D \overline{C}_v \tag{29}$$

$$\overline{C}_T = K_d C_T \overline{C}_v \tag{30}$$

and since,

$$\overline{C}_m = \overline{C}_v + \overline{C}_G + \overline{C}_B + \overline{C}_M + \overline{C}_D + \overline{C}_T \tag{31}$$

Therefore, by assuming the surface reaction controls and combining Eqs. (9), (15), (16), (17), and (18), it yields:

$$\overline{C}_v = \frac{\overline{C}_m}{1 + K_G C_G + K_B C_B + k_d(C_M + C_D + C_T)} \quad (32)$$

Substituting for $\overline{C}_v$, the rate of surface reaction will be expressed as:

$$rate = r_s = \frac{\overline{C}_v^2}{\overline{C}_m}\left(K_G K_B C_G C_B - \frac{k_d(C_M + C_D + C_T)}{K_s}\right) \quad (33)$$

The value of C_v depends on the surface acidity, and will be given by

$$\frac{C_G}{C_{Gs}} = \frac{r_s}{r}\frac{Sinh(3\varphi_s r/r_s)}{Sinh(3\varphi_s)} \quad (34)$$

where

$$\varphi_s = \frac{r_s}{3}\sqrt{\frac{k_1\rho_p}{D_e}} \quad (35)$$

φ_s is the thiele-type modulus for spherical particle pellet, k_1 is the pseudo-first order rate constant, ρ_p is particle density (g/cm^3). Since the effectiveness factor (η) represents the ratio between the reaction rate for pellet (r_p) and the diffusion rate of reactant into the pellet (r_s), then $r_p = \eta\, r_s$ or $r_p = \eta\, k_1 C_{Gs}$. Thus, the following model would be generated:

$$\eta = \frac{1}{\varphi_s}\left(\frac{1}{tanh3\varphi_s} - \frac{1}{3\varphi_s}\right) \quad (36)$$

Based on the above equation, the r_p can be obtained from $r_p = \eta\, k_1 C_{Gs}$ as;

$$r_p = \frac{1}{\varphi_s}\left(\frac{1}{tanh3\varphi_s} - \frac{1}{3\varphi_s}\right)k_1 C_{Gs} \quad (37)$$

The controlling resistance was evaluated based on the relative magnitude of mass transfer coefficient k_m obtained from Eq. (6), η, and k_1. The kinetics and thermodynamics parameters were calculated for the acetylation process at the optimized reaction conditions using POLYMATH 5.1 software. These values and other important parameters are summarized in Table 3.

In accordance with the assumptions made, that are: (i) The sites on the catalyst surface are the same; (ii) The rate of uncatalyzed reaction is slower than the catalyzed one and thus its neglected; (iii) The surface reaction is the rate limiting step (Eq. (33)); and (v) The adsorption and desorption of the reactants and the products were faster and at equilibrium. Thus, the reaction rate equation in the rate controlling step could be expressed as:

$$rate = r_s = \frac{\overline{C}_v^2}{\overline{C}_m}\left(K_G K_B C_G C_B - \frac{k_d(C_M + C_D + C_T)}{K_s}\right) \quad (38)$$

4. Conclusions

The selective acetylation of glycerol with acetic acid was performed over a series of heterogeneous catalysts, prepared by grafting yttrium (1–3.5 wt.%) into the framework of SBA-3 support. The 3%Y/SBA-3 catalyst exhibited the best catalytic activity achieving complete glycerol conversion with corresponding selectivity of 11%, 34% and 55% toward MAG, DAG and TAG, respectively. The economized reaction conditions are; 110 °C, molar ratio of glycerol/acetic acid of 1:4, and 2.5 h. The catalytic performance of 3%Y/SBA-3 catalyst should be attributed to its strong acidity and high surface area with large pore size that facilitated the diffusion of substrates and products. The reusability tests confirmed the stability of the catalytic activity of the 3%Y/SBA-3 catalyst. The characterization results of the spent 3%Y/SBA-3 catalyst unveiled no serious changes to the structural and chemical characteristics. It is therefore recommended to scale up this process for industrial applications.

Acknowledgements

The authors gratefully acknowledge the financial support provided by the Universiti Sains Malaysia. Also, the authors extend their deep thanks to the Universiti Teknologi Malaysia for the Visiting Researcher (Publication) Scheme.

References

[1] J.A. Melero, J. Iglesias, G. Morales, Heterogeneous acid catalysts for biodiesel production: current status and future challenges, Green Chem. 11 (2009) 1285–1308.
[2] M.S. Khayoon, M.A. Olutoye, B.H. Hameed, Utilization of crude karanj (*Pongamia pinnata*) oil as a potential feedstock for the synthesis of fatty acid methyl esters, Bioresour. Technol. 111 (2012) 175–179.
[3] M. Balaraju, P. Nikhitha, K. Jagadeeswaraiah, K. Srilatha, P.S. Sai Prasad, N. Lingaiah, Acetylation of glycerol to synthesize bioadditives over niobic acid supported tungstophosphoric acid catalysts, Fuel Proc. Technol. 91 (2010) 249–253.
[4] S. Zhu, Y. Zhu, S. Hao, H. Zheng, T. Mo, Y. Li, One-step hydrogenolysis of glycerol to biopropanols over Pt–$H_4SiW_{12}O_{40}/ZrO_2$ catalysts, Green Chem. 14 (2012) 2607–2616.
[5] R.P.V. Faria, C.S.M. Pereira, V.M.T.M. Silva, J.M. Loureiro, A.E. Rodrigues, Glycerol valorisation as biofuels: selection of a suitable solvent for an innovative process for the synthesis of GEA, Chem. Eng. J. 233 (2013) 159–167.
[6] F.F. de Sousa, A.C. Oliveira, J.M. Filho, G.S. Pinheiro, M. Giotto, N.A. Barros, H.S.A. Souza, A.C. Oliveira, Metal oxides nanoparticles from complexes on SBA-15 for glycerol conversion, Chem. Eng. J. 228 (2013) 442–448.
[7] L. Shen, H. Yin, A. Wang, Y. Feng, Y. Shen, Z. Wu, T. Jiang, Liquid phase dehydration of glycerol to acrolein catalyzed by silicotungstic, phosphotungstic, and phosphomolybdic acids, Chem. Eng. J. 180 (2012) 277–283.
[8] X. Liu, H. Ma, Y. Wu, C. Wang, M. Yang, P. Yan, U. Welz-Biermann, Esterification of glycerol with acetic acid using double SO_3H-functionalized ionic liquids as recoverable catalysts, Green Chem. 13 (2011) 697–701.
[9] E.S. Vasiliadou, A.A. Lemonidou, Kinetic study of liquid-phase glycerol hydrogenolysis over Cu/SiO_2 catalyst, Chem. Eng. J. 231 (2013) 103–112.
[10] M.B. Güemez, J. Requies, I. Agirre, P.L. Arias, V.L. Barrio, J.F. Cambra, Acetalization reaction between glycerol and n-butyraldehyde using an acidic ion exchange resin. Kinetic modelling, Chem. Eng. J. 228 (2013) 300–307.
[11] N. Rahmat, A.Z. Abdullah, A.R. Mohamed, Recent progress on innovative and potential technologies for glycerol transformation into fuel additives: a critical review, Ren. Sus. Energy Rev. 14 (2010) 987–1000.
[12] K. Jagadeeswaraiah, M. Balaraju, P.S.S. Prasad, N. Lingaiah, Selective esterification of glycerol to bioadditives over heteropoly tungstate supported on Cs-containing zirconia catalysts, Appl. Catal. A: Gen. 386 (2010) 166–170.
[13] M.L. Testa, V. La Parola, L.F. Liotta, A.M. Venezia, Screening of different solid acid catalysts for glycerol acetylation, J. Mol. Catal. A: Chem. 367 (2013) 69–76.
[14] M.S. Khayoon, B.H. Hameed, Yttrium-grafted mesostructured SBA-3 catalyst for the transesterification of glycerol with methyl acetate to synthesize fuel oxygenates, Appl. Catal. A: Gen. 460–461 (2013) 61–69.
[15] W.Y. Jung, G.D. Lee, S.S. Park, K.T. Lim, S.-S. Hong, Photocatalytic decomposition of methylene blue over yttrium ion doped Ti-SBA-15 catalysts, Catal Today 164 (2011) 395–398.
[16] O.A. Anunziata, A.R. Beltramone, M.L. Martínez, L.L. Belon, Synthesis and characterization of SBA-3, SBA-15, and SBA-1 nanostructured catalytic materials, J. Colloid Interface Sci. 315 (2007) 184–190.
[17] M. Ziolek, I. Nowak, B. Kilos, I. Sobczak, P. Decyk, M. Trejda, J.C. Volta, Template synthesis and characterisation of MCM-41 mesoporous molecular sieves containing various transition metal elements-TME (Cu, Fe, Nb, V, Mo), J. Phys. Chem. Sol. 65 (2004) 571–581.
[18] Y. Li, X. Lin, Y. Wang, J. Luo, W. Sun, Preparation and characterization of porous yttrium oxide powders with high specific surface area, J. Rare Ear. 24 (2006) 34–38.
[19] M. Anbia, S. Salehi, Removal of acid dyes from aqueous media by adsorption onto amino-functionalized nanoporous silica SBA-3, Dyes Pig. 94 (2012) 1–9.
[20] L. Zhou, E. Al-Zaini, A.A. Adesina, Catalytic characteristics and parameters optimization of the glycerol acetylation over solid acid catalysts, Fuel 103 (2013) 617–625.
[21] M.S. Khayoon, B.H. Hameed, Synthesis of hybrid SBA-15 functionalized with molybdophosphoric acid as efficient catalyst for glycerol esterification to fuel additives, Appl. Catal. A: Gen. 433–434 (2012) 152–161.
[22] M.S. Khayoon, B.H. Hameed, Acetylation of glycerol to biofuel additives over sulfated activated carbon catalyst, Bioresour. Technol. 102 (2011) 9229–9235.
[23] X. Liao, Y. Zhu, S.-G. Wang, H. Chen, Y. Li, Theoretical elucidation of acetylating glycerol with acetic acid and acetic anhydride, Appl. Catal. B: Environ. 94 (2010) 64–70.

[24] M. Trejda, K. Stawicka, M. Ziolek, New catalysts for biodiesel additives production, Appl. Catal. B: Environ. 103 (2011) 404–412.
[25] J.A. Melero, G. Vicente, G. Morales, M. Paniagua, J. Bustamante, Oxygenated compounds derived from glycerol for biodiesel formulation: influence on EN 14214 quality parameters, Fuel 89 (2010) 2011–2018.
[26] H.-P. Lin, C.-Y. Chang-Chien, C.-Y. Tang, C.-Y. Lin, Synthesis of p6mm hexagonal mesoporous carbons and silicas using Pluronic F127–PF resin polymer blends, Microporous Mesoporous Mater. 93 (2006) 344–348.
[27] S. Pikus, L.A. Solovyov, M. Kozak, M. Jaroniec, Comparative studies of p6m siliceous mesostructures by powder X-ray diffraction and nitrogen adsorption, Appl. Surf. Sci. 253 (2007) 5682–5687.
[28] C.E. Gonçalves, L.O. Laier, M.J. da Silva, Novel esterification of glycerol catalysed by tin chloride (II): a recyclable and less corrosive process for production of bio-additives, Catal. Lett. 141 (2011) 1111–1117.
[29] L.N. Silva, V.L.C. Gonçalves, C.J.A. Mota, Catalytic acetylation of glycerol with acetic anhydride, Catal. Commun. 11 (2010) 1036–1039.
[30] M. Pagliaro, R. Ciriminna, H. Kimura, M. Rossi, C. Della Pina, Ang. Chem. Int. Ed. 46 (2007) 4434–4440.
[31] Ó. de la Iglesia, R. Mallada, M. Menéndez, J. Coronas, Continuous zeolite membrane reactor for esterification of ethanol and acetic acid, Chem. Eng. J. 131 (2007) 35–39.
[32] S.R. Kirumakki, N. Nagaraju, S. Narayanan, A comparative esterification of benzyl alcohol with acetic acid over zeolites H, HY and HZSM5, Appl. Catal. A: Gen. 273 (2004) 1–9.
[33] I. Dosuna-Rodríguez, C. Adriany, E.M. Gaigneaux, Glycerol acetylation on sulphated zirconia in mild conditions, Catal. Today. 167 (2011) 56–63.
[34] Z. Mufrodi, Rochmadi Sutijan, A. Budiman, Chemical kinetics for synthesis of triacetin from biodiesel byproduct, Int. J. Chem. 4 (2012) 101–107.
[35] L. Zhou, T.-H. Nguyen, A.A. Adesina, The acetylation of glycerol over amberlyst-15: kinetic and product distribution, Fuel Proc. Technol. 104 (2012) 310–318.